Electronic Supplementary Material (ESI) for Journal of Materials Chemistry A.

Hierarchical core-shell structural $NiMoO_4$@NiS_2/MoS_2 nanowires fabricated via in-situ sulfurization method for high performance asymmetric supercapacitor

Duo Chen,[a]† Mengjie Lu,[a]† La Li,*[a] Dong Cai,[a] Junzhi Li,[a] Junming Cao[a] and Wei Han*[a,b]

[a] Sino-Russian International Joint Laboratory for Clean Energy and Energy Conversion Technology, College of Physics, Jilin University, Changchun 130012, P. R. China. E-mail: lali910217@gmail.com; whan@jlu.edu.cn

[b] International Center of Future Science, Jilin University, Changchun City 130012, PR China.

† These authors contributed equally to this work.

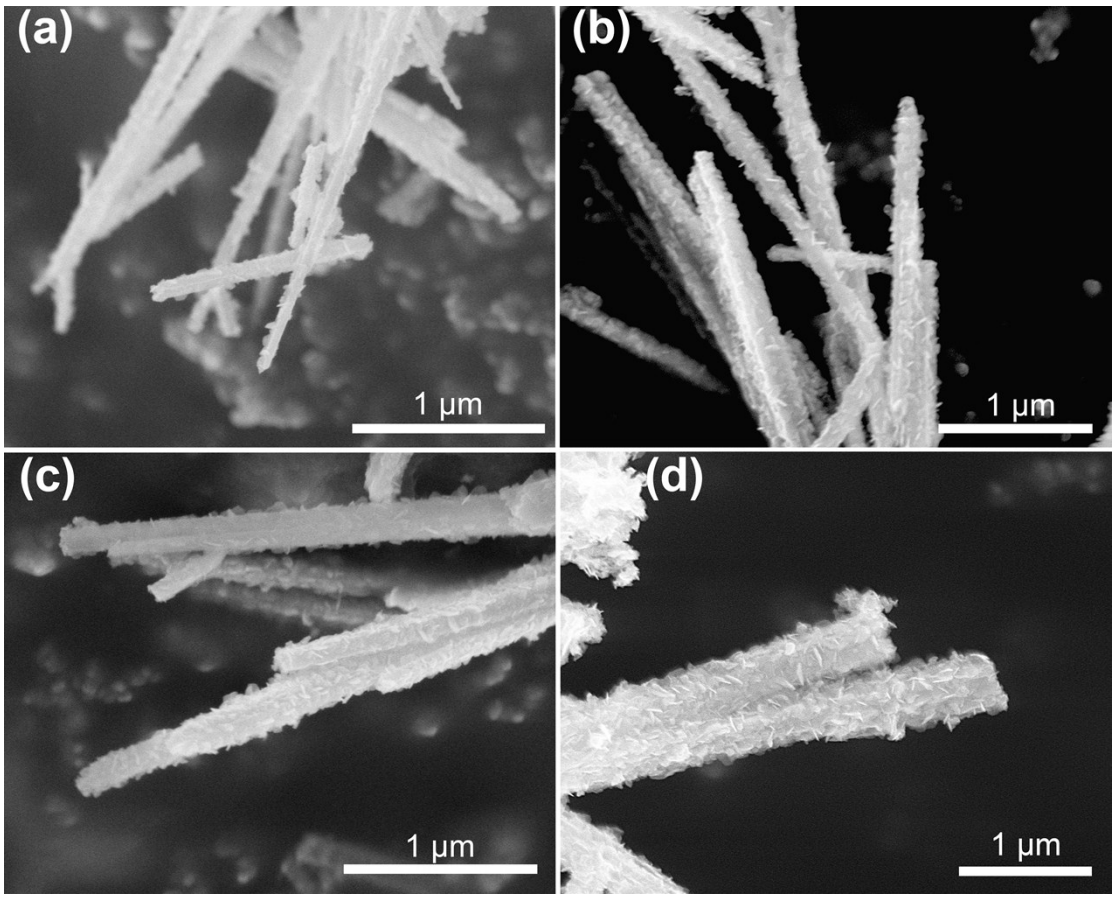

Fig. S1 The morphology evolution of as-obtained samples as sulfur mass increasing in the preparation process: (a) S-$NiMoO_4$-1; (b) S-$NiMoO_4$-2; (c) S-$NiMoO_4$-3; (d) NiS_2/MoS_2.

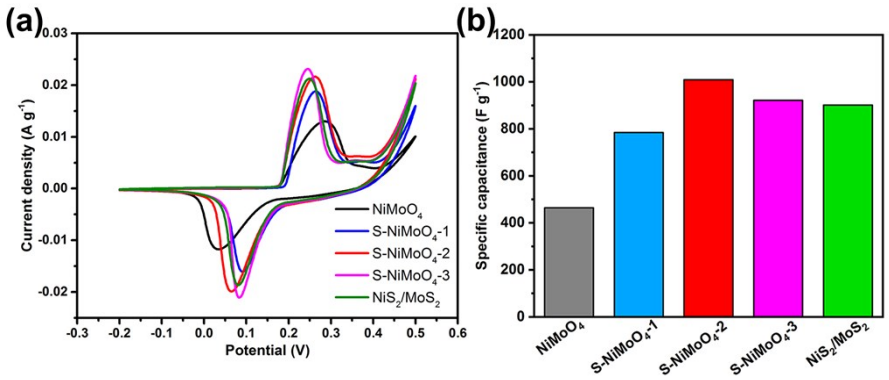

Fig. S2 (a) CV curves of different samples at a same scan rate of 5 mV s^{-1} and (b) calculated specific capacitance at this scan rate corresponding to (a).

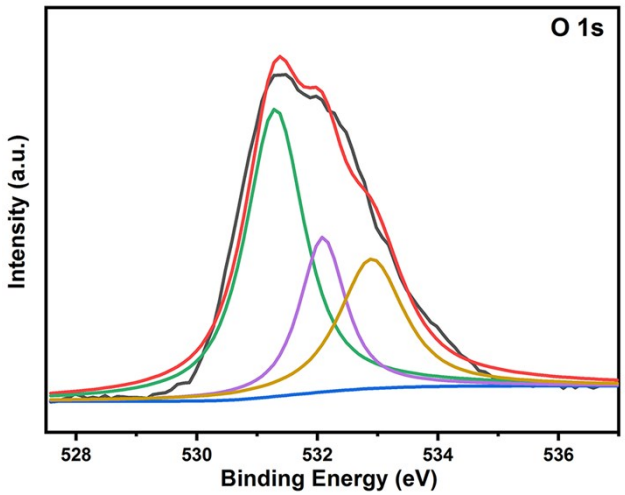

Fig. S3 High resolution XPS spectrum of O 1s in S-$NiMoO_4$-2 nanowires.

Table S1 The detailed data of various samples obtained by GCD profiles

Samples	**Specific capacitance obtained by GCD profiles (F g^{-1})**				
	5 A g^{-1}	7.5 A g^{-1}	10 A g^{-1}	15 A g^{-1}	20 A g^{-1}
$NiMoO_4$	407	363	329	267	213
S-$NiMoO_4$-1	707	633	591	473	409
S-$NiMoO_4$-2	970	897	844	780	711
S-$NiMoO_4$-3	833	773	733	673	631
NiS_2/MoS_2	761	682	607	533	476

Table S2 The specific capacities of various samples

Samples	**Specific capacities (C g^{-1})**				
	5 A g^{-1}	7.5 A g^{-1}	10 A g^{-1}	15 A g^{-1}	20 A g^{-1}
$NiMoO_4$	183	163	148	120	96
S-$NiMoO_4$-1	318	285	266	213	184
S-$NiMoO_4$-2	437	404	380	351	320
S-$NiMoO_4$-3	375	348	330	303	284
NiS_2/MoS_2	343	307	273	240	214

Table S3 The detailed data of various samples obtained by CV curves

Samples	**Specific capacitance obtained by CV curves (F g^{-1})**					
	5 mV s^{-1}	10 mV s^{-1}	15 mV s^{-1}	20 mV s^{-1}	30 mV s^{-1}	50 mV s^{-1}
$NiMoO_4$	464	398	380	363	331	267
S-$NiMoO_4$-1	784	627	573	538	497	436
S-$NiMoO_4$-2	1010	805	742	704	654	579
S-$NiMoO_4$-3	921	727	660	622	578	523
NiS_2/MoS_2	901	660	586	543	492	427

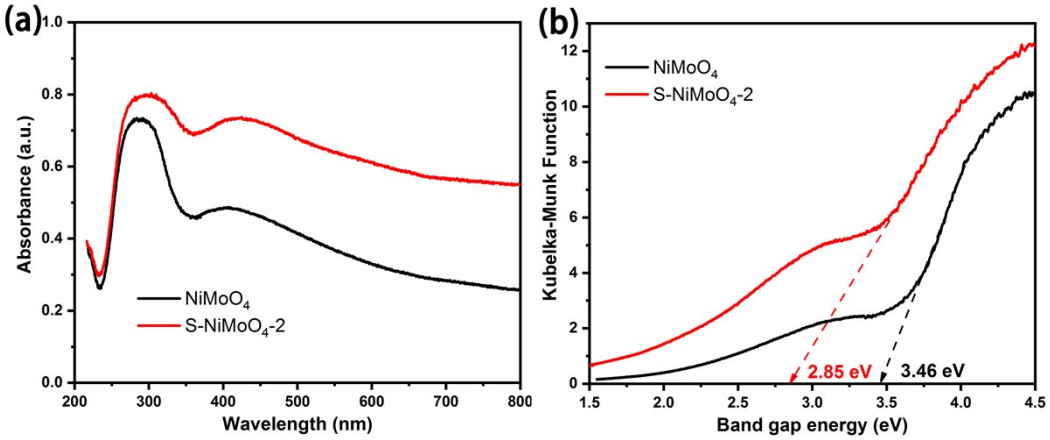

Fig. S4 (a) UV-Vis diffuse reflectance spectra and (b) Kubelka-Munk plot for estimating bandgap energy of $NiMoO_4$ and S-$NiMoO_4$-2.

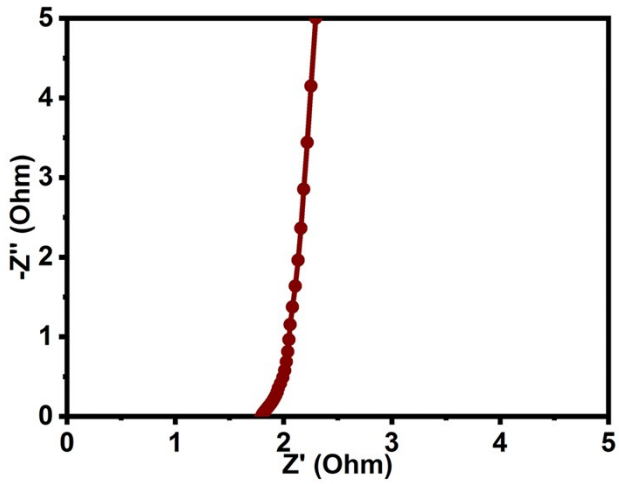

Fig. S5 Electrochemical impedance spectrum of the S-$NiMoO_4$-2 based ASC.

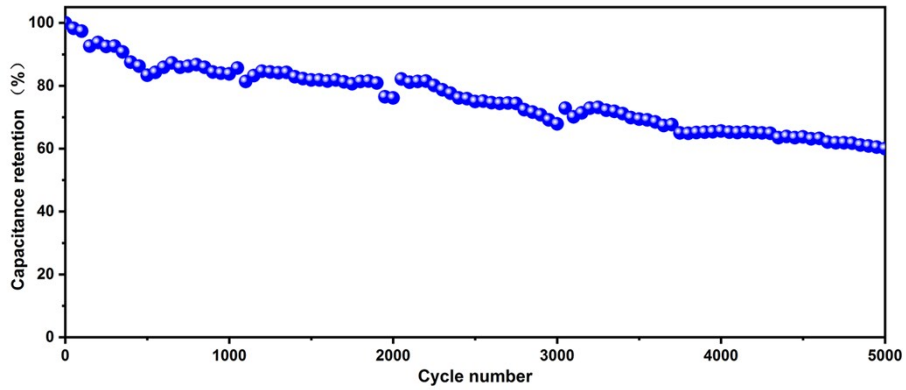

Fig. S6 Cycling stability of the S-$NiMoO_4$-2 based ASC at a fixed current density of 2 A g^{-1}.

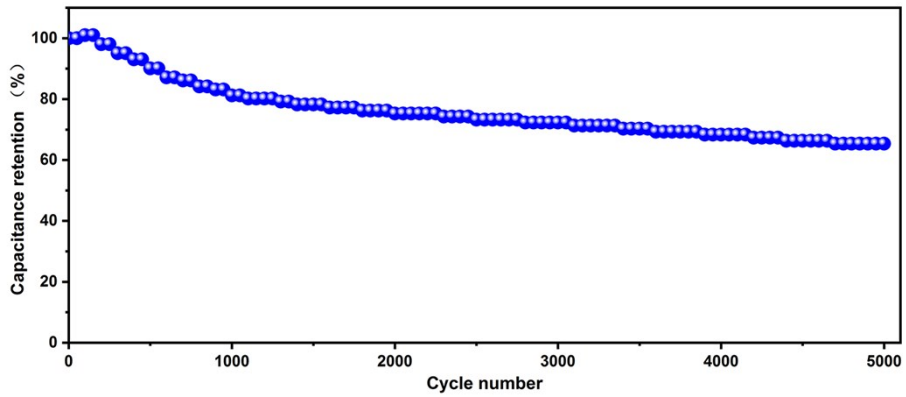

Fig. S7 Cycling stability of S-$NiMoO_4$-2 electrode in a 3-electrode system at a current density of 15 A g^{-1}. The S-$NiMoO_4$-2 electrode can deliver more than 65.3% capacitance after 5000 cycles.

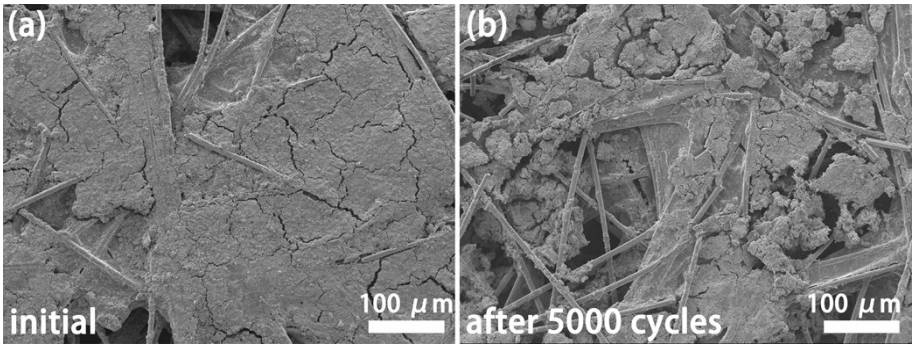

Fig. S8 SEM images of (a) the initial S-$NiMoO_4$-2 electrode and (b) the electrode after 5000 cycles in 6 M KOH. The fiber-shape matters are carbon fiber of the carbon paper substrate.